State-space model of grid-connected inverters under current control mode

N. Kroutikova, C.A. Hernandez-Aramburo and T.C. Green

Abstract: Growth of distributed generation has led to distribution systems with a mixture of rotating machine generators and inverter interfaced generators. The stability of such networks needs to be studied through the analysis of state-space models, and so suitable models of inverters are needed to complement the well-established models of rotating machines. As machine models include features such as automatic voltage regulators and wash-out functions, the inverter model also includes phase-locking functions and internal control loops. The model for voltage source inverters with an internal current control loop, an outer power regulation loop, a measurement of average power and a phase-locked loop has been developed. The model is presented in detail and is formed with a state-vector, similar to that used for rotating machines. The model includes nonlinear terms but can be linearised about an operating point. The state-space model is verified against a component-level time-step simulation in Simulink/PLECS.

1 Introduction

Many of the forms of new and renewable energy are not natural 50 or 60 Hz sources and the question arises of how to incorporate them into a standard electricity grid. Most of this technology (PV panels, high-speed microturbines and fuel cells) has an inverter as a generator interface. That inverter can operate either as a current source or as a voltage source is generally known. In either case, the implementation will normally be a voltage source inverter (VSI) and appropriate control loops will be added to make it appear as a controlled current source, if necessary. The inverter will be fitted with a coupling impedance and possibly further passive filter elements to attenuate the switching frequency components of voltage. The inverter will also require a means to measure exported power. The inverter must also be explicitly phase-locked through a phase-locked loop (PLL) or implicitly phase-locked through droop regulation. Thus, the inverter is a complex dynamic system, which interacts with the grid. In some circumstances, it will be necessary to establish the stability limits of the inverter and grid combination. For traditional generators, such as synchronous machines and induction (asynchronous) machines, there are well-established dynamic models, and for each type of stability study (covering various frequency ranges and types of interaction) an appropriate model can be selected that includes all of the necessary machine features and has a standard state vector. Many years of experience and design standardisation has led to the situation where power systems engineers know the appropriate features and modes to be included in each type of study. Inverter-interfaced generators are not yet that mature and the modelling of inverters for network stability studies requires much more work, if grid stability is to be ensured with high penetrations of distributed generation (DG).

Component-level models (e.g. Spice-based simulators) allow the evaluation of inverter performance during every switching action [1]. Applications at this level of simulation detail include the calculation of switching losses and the testing of snubber networks [2]. This simulation approach offers an accurate representation of the system in the time domain but it can be highly time consuming to perform over the duration of a power frequency oscillation. Another approach to simulate the switching action of the power devices is to use the principle of switching functions [3, 4]. A disadvantage of this approach is that the switching instants of the devices must be known in advance. At the other end of the spectrum (in terms of the simulation detail to be used), there are applications in which modelling the whole inverter system as a simple voltage gain is good enough. In these applications, the inverter is normally a small part of a large system and the dynamics of the inverter have a small impact on the overall system.

Inverters are sometimes modelled in a space-state formulation with the power devices in the inverter represented as ideal switches [5]. Under this assumption, some accuracy is lost but the simulation time is normally improved by reducing both the time required by an analyst to set up a simulation and the time taken by a computer to produce the result. Space-state modelling of power converters is well documented in textbooks [6] and it has been used to simulate many different types of power converters. A common simplification is to linearise the switching circuit by creating a small-signal model and to consider the average behaviour of the switched circuit over a period. A small sample of the literature includes: DC–DC converters [7], AC–DC converters [8–10], DC–AC converters [11–14] and FACTS devices [15].

Despite the modelling efforts, to date, better VSI models are still needed for studies of DG integration. The model must represent all of the dynamics of the inverter in the frequency range of interest and allow coupling to reasonable

© The Institution of Engineering and Technology 2007

doi:10.1049/iet-epa:20060276

Paper first received 15th May and in revised form 31st October 2006

The authors are with the Department of Electrical and Electronic Engineering, Imperial College London, London, SW7 2BT, UK

E-mail: c.a.hernandez@imperial.ac.uk

models of the distribution network. Models of VSIs for grid connection, normally, include the low pass (LC-based) filter required to attenuated switching frequency noise and the coupling impedance between the filter and connection node, in the distribution network. A complete model should also include the control system associated with the converter circuit [16–20]. This includes the PLL, the abc–dq transformations, the controllers for current and voltage and any low-pass filters applied to feedback or control signals (such as those used to obtain average power from instantaneous power or to attenuate noise in measured signals).

This paper presents a model of a three-phase inverter system, including a complete set of the sub-systems required for interfacing a DG source to a grid. The model is for current-control mode, which is one of the two main operation modes relevant to DG. It is presented in detail so that the meaning of the various parameters can be understood and can be related to features of real inverters. The validation of the model is carried out by comparing waveforms generated from the state-space model with those from a component level simulation in Simulink/PLECS.

The intended contribution of this paper is to provide verified models of inverter-interfaced generators to be used by a wider community by studying interactions between inverters and the power system to which they are connected.

2 VSI in current control mode

In situations where a strong network connection is available, that is, a connection point with an already tightly regulated voltage and frequency, it is common to export power into that connection through setting a current reference for the inverter. That reference can represent any combination of real and reactive power needs to be understood. The exported power will not significantly influence the voltage or frequency at the point of connection. A schematic of an inverter arranged in current-controlled mode is shown in Fig. 1 and follows the proposal made in [21]. The objective is to regulate real and reactive power to follow reference values (P^* and Q^*). The power references and the voltages at the point of connection (v_{Oa}, v_{Ob}, and v_{Oc}) are used to set references for the current controllers. The inverter is provided with a DC link voltage (V_{DC}) from the original energy source. These variables constitute the inputs to the model. The output variables of direct interest are the output currents (i_{Oa}, i_{Ob} and i_{Oc}). It might also be desirable to monitor the alignment angle of the PLL or, if the model is to be coupled to a model of the energy source, the DC link current (i_{DC}) can be arranged as an output. Fig. 1 shows that control is performed in a rotating reference frame (dq domain) and the reference angle for the abc–dq transformation is provided by the PLL. The inverter output is shown with a second-order LC element and an additional inductor for coupling to the connection point. The output current (i_{Odq}) is therefore equal to the current in the filter inductor minus the current in the shunt-connected capacitor of the filter. It is the inductor current i_L, which is controlled to follow the reference current (in turn determined by the power references) [22]. It is assumed that the current in the filter capacitor is of high frequency and, in terms of power export at fundamental frequency, the inductor and output currents are essentially identical. Other variables shown in Fig. 1 will be discussed in detail as the paper progresses.

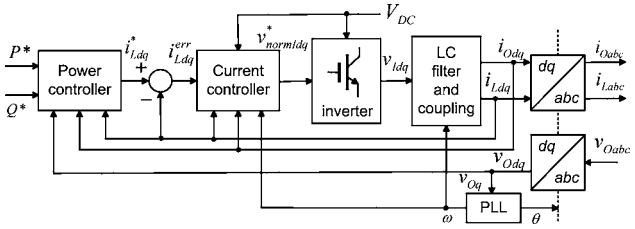

Fig. 1 *Model of a current-controlled VSI*

The objective is to build a single state-space model for all of the elements shown in Fig. 1 such that the dynamics of both the power processing elements and the associated local controls are included. This model will be of the form described by (1), which is a state-space form that allows nonlinear functions of x and u to be included. To accomplish this goal, in the following sub-sections a state-space model is derived for each sub-system. The sub-system models are, then, arranged into a complete model and duplicate variables eliminated

$$\dot{\boldsymbol{x}} = \boldsymbol{A}\boldsymbol{x} + \boldsymbol{R}(\boldsymbol{x}, \boldsymbol{u})$$
$$\boldsymbol{y} = \boldsymbol{S}(\boldsymbol{x}, \boldsymbol{u}) \tag{1}$$

2.1 State-space model of the dq–abc transformation

The first sub-system in the inverter topology is the dq–abc transformation as defined by (2).

$$\begin{bmatrix} i_{\mathrm{Oa}} \\ i_{\mathrm{Ob}} \\ i_{\mathrm{Oc}} \end{bmatrix} = \sqrt{\frac{2}{3}} \begin{bmatrix} \cos\theta & -\sin\theta & \frac{1}{\sqrt{2}} \\ \cos\left(\theta - \frac{2\pi}{3}\right) & -\sin\left(\theta - \frac{2\pi}{3}\right) & \frac{1}{\sqrt{2}} \\ \cos\left(\theta + \frac{2\pi}{3}\right) & -\sin\left(\theta + \frac{2\pi}{3}\right) & \frac{1}{\sqrt{2}} \end{bmatrix} \begin{bmatrix} i_{\mathrm{Od}} \\ i_{\mathrm{Oq}} \\ i_{\mathrm{Oo}} \end{bmatrix} \tag{2}$$

The angle of the rotational frame is treated as an input to this sub-system and there are no state variables. Equation (2) represents a feed-through term from input to output and no state-vector is needed

$$\dot{\boldsymbol{x}}_1 = [0] \tag{3}$$

2.2 State-space model of the PLL system

The PLL system indicated in Fig. 1 is given in more detail in Fig. 2.

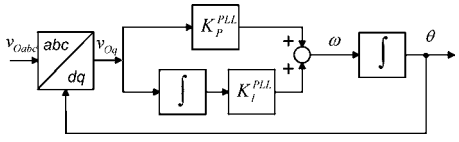

Fig. 2 *Model for the PLL*

The abc–dq transformation is defined by (4)

$$\begin{bmatrix} v_{\mathrm{Od}} \\ v_{\mathrm{Oq}} \\ v_{\mathrm{Oo}} \end{bmatrix} = \sqrt{\frac{2}{3}} \begin{bmatrix} \cos\theta & \cos\left(\theta - \frac{2\pi}{3}\right) & \cos\left(\theta + \frac{2\pi}{3}\right) \\ -\sin\theta & -\sin\left(\theta - \frac{2\pi}{3}\right) & -\sin\left(\theta + \frac{2\pi}{3}\right) \\ \frac{1}{\sqrt{2}} & \frac{1}{\sqrt{2}} & \frac{1}{\sqrt{2}} \end{bmatrix} \times \begin{bmatrix} v_{\mathrm{Oa}} \\ v_{\mathrm{Ob}} \\ v_{\mathrm{Oc}} \end{bmatrix} \tag{4}$$

In this paper, it is assumed that there is no path for the zero sequence components, therefore $i_{\mathrm{O_o}}$ in (2) and $v_{\mathrm{O_o}}$ in (4) could be ignored. However, these variables are left in the formulation to pave the way for a more general case.

The PLL form adopted here is based on aligning in closed-loop control the angle of the dq-transformation such that the voltage at the connection point has no q-axis component [23]. A PI regulator acts on the alignment error to set the rotation frequency (5) and that frequency is integrated to give the transformation angle (6).

$$\omega = K_{\mathrm{P}}^{\mathrm{PLL}} v_{\mathrm{Oq}} + K_{\mathrm{I}}^{\mathrm{PLL}} \int v_{\mathrm{Oq}}\, \mathrm{d}t \tag{5}$$

$$\theta = \int \omega\, \mathrm{d}t \tag{6}$$

To express (5) in a purely differential form, an additional variable is defined: $\Phi_{\mathrm{PLL}} = \int v_{\mathrm{Oq}}\, \mathrm{d}t$. This variable does not have a particular physical meaning but it facilitates the development of the state-space model (and has the same dimensions as magnetic flux). The additional variable is a part of the state-vector together with θ (taken from (6)): $\boldsymbol{x}_2 = \begin{bmatrix} \theta & \Phi_{\mathrm{PLL}} \end{bmatrix}^{\mathrm{T}}$. The input variable to the PLL is $\boldsymbol{u}_2 = \begin{bmatrix} v_{\mathrm{Oa}} & v_{\mathrm{Ob}} & v_{\mathrm{Oc}} \end{bmatrix}^{\mathrm{T}}$ and the output, which includes the dq transformation, is $\boldsymbol{y}_2 = \begin{bmatrix} \theta & v_{\mathrm{Od}} & v_{\mathrm{Oq}} \end{bmatrix}^{\mathrm{T}}$.

With the above definitions, the state-space model of PLL loop can then be written in the form $\dot{\boldsymbol{x}}_2 = \boldsymbol{A}_2\boldsymbol{x}_2 + \boldsymbol{R}_2(\boldsymbol{x}_2, \boldsymbol{u}_2)$ as follows

$$\dot{\boldsymbol{x}}_2 = \begin{bmatrix} 0 & K_{\mathrm{T}}^{\mathrm{PLL}} \\ 0 & 0 \end{bmatrix} \begin{bmatrix} 0 \\ \Phi_{\mathrm{PLL}} \end{bmatrix} + \begin{bmatrix} K_{\mathrm{P}}^{\mathrm{PLL}} v_{\mathrm{Oq}} \\ v_{\mathrm{Oq}} \end{bmatrix} \tag{7}$$

where v_{Oq} is given in (4) and is a multiplication of state θ with input v_{Oabc}.

2.3 State-space model of the power controller

The power controller is not a closed-loop controller but instead is an open-loop conversion of a power reference into a current reference, given the prevailing voltage at the point of connection. The current is then controlled in closed-loop as given in the next section. This sub-system is nonlinear because of the need to divide power by voltage to obtain current and it contains higher-order dynamics because of the filter employed. The sub-system is illustrated in Fig. 3.

The desired output currents are calculated using the following pair of equations

$$i_{\mathrm{Od}}^{*} = \frac{v_{\mathrm{Od}}P^{*} - v_{\mathrm{Oq}}Q^{*}}{v_{\mathrm{Od}}^2 + v_{\mathrm{Oq}}^2} \qquad i_{\mathrm{Oq}}^{*} = \frac{v_{\mathrm{Oq}}P^{*} + v_{\mathrm{Od}}Q^{*}}{v_{\mathrm{Od}}^2 + v_{\mathrm{Oq}}^2} \tag{8}$$

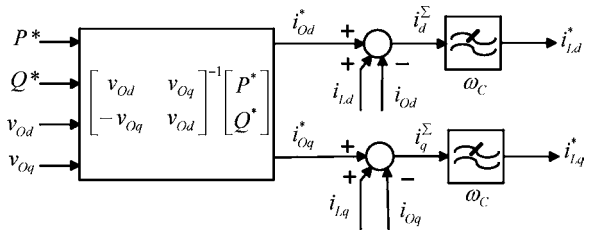

Fig. 3 *Power controller [22]*

It is actually the filter inductor current that is controlled and so an adjustment must be made to the reference to account for the capacitor current. This is performed using the measured inductor current and measured output current

$$\begin{aligned} i_d^{\Sigma} &= i_{\mathrm{Od}}^{*} + i_{\mathrm{Cd}} = i_{\mathrm{Od}}^{*} + (i_{\mathrm{Ld}} - i_{\mathrm{Od}}) \\ i_q^{\Sigma} &= i_{\mathrm{Oq}}^{*} + i_{\mathrm{Cq}} = i_{\mathrm{Oq}}^{*} + (i_{\mathrm{Lq}} - i_{\mathrm{Oq}}) \end{aligned} \tag{9}$$

These current references might contain harmonic and noise terms as a consequence of distortion of the voltage at the point of connection. These are removed from the reference by a low-pass filter. Because of the relatively low cut-off frequency required of this filter it can make an important contribution to the dynamics of the system and should be included in the model. A second-order Butterworth low-pass transfer function is taken as a representative of the filter likely to be used. Equation (10) shows the references for the current controllers, i_{Ld}^{*} and i_{Lq}^{*}, formed by the product of a generic filter and the terms in (9)

$$\begin{aligned} i_{\mathrm{Ld}}^{*} &= \frac{\omega_{\mathrm{c}}^2}{s^2 + \sqrt{2}s\omega_{\mathrm{c}} + \omega_{\mathrm{c}}^2} i_d^{\Sigma}, \\ i_{\mathrm{Lq}}^{*} &= \frac{\omega_{\mathrm{c}}^2}{s^2 + \sqrt{2}s\omega_{\mathrm{c}} + \omega_{\mathrm{c}}^2} i_{\mathrm{q}}^{\Sigma} \end{aligned} \tag{10}$$

Equation (10) can be re-arranged as in (11) and then re-written in integro-differential form as in (12)

$$\begin{aligned} i_{\mathrm{Ld}}^{*}s + i_{\mathrm{Ld}}^{*}\sqrt{2}\omega_{\mathrm{c}} + i_{\mathrm{Ld}}^{*}\frac{1}{s}\omega_{\mathrm{c}}^2 &= \frac{1}{s}\omega_{\mathrm{c}}^2 i_{\mathrm{d}}^{*} \\ i_{\mathrm{Lq}}^{*}s + i_{\mathrm{Lq}}^{*}\sqrt{2}\omega_{\mathrm{c}} + i_{\mathrm{Lq}}^{*}\frac{1}{s}\omega_{\mathrm{c}}^2 &= \frac{1}{s}\omega_{\mathrm{c}}^2 i_{\mathrm{q}}^{*} \end{aligned} \tag{11}$$

$$\begin{aligned} \frac{\mathrm{d}i_{\mathrm{Ld}}^{*}}{\mathrm{d}t} &= \omega_{\mathrm{c}}^2 \int (i_{\mathrm{d}}^{\Sigma} - i_{\mathrm{Ld}}^{*})\, \mathrm{d}t - \omega_{\mathrm{c}}\sqrt{2}\, i_{\mathrm{Ld}}^{*} \\ &= \omega_{\mathrm{c}}^2 q_{3\mathrm{d}} - \omega_{c}\sqrt{2}\, i_{\mathrm{Ld}}^{*} \\ \frac{\mathrm{d}i_{\mathrm{Lq}}^{*}}{\mathrm{d}t} &= \omega_{\mathrm{c}}^2 \int (i_{\mathrm{q}}^{\Sigma} - i_{\mathrm{Lq}}^{*})\, \mathrm{d}t - \omega_{\mathrm{c}}\sqrt{2}\, i_{\mathrm{Lq}}^{*} \\ &= \omega_{\mathrm{c}}^2 q_{3\mathrm{q}} - \omega_{\mathrm{c}}\sqrt{2}\, i_{\mathrm{Lq}}^{*} \end{aligned} \tag{12}$$

Equations (8), (9) and (12) together describe the power controller. They can be assembled into state-space form by introducing new variables for the integrals in (12). Since these are integrations of current, the new variables are denoted as charges: $q_{3\mathrm{d}} = \int (i_{\mathrm{d}}^{\Sigma} - i_{\mathrm{Ld}}^{*})\, \mathrm{d}t$ and $q_{3\mathrm{q}} = \int (i_{\mathrm{q}}^{\Sigma} - i_{\mathrm{Lq}}^{*})\, \mathrm{d}t$. The state-variable is then

$\boldsymbol{x}_3 = \begin{bmatrix} i^*_{\mathrm{Ld}} & i^*_{\mathrm{Lq}} & q_{3\mathrm{d}} & q_{3\mathrm{q}} \end{bmatrix}^{\mathrm{T}}$ and the input vector is $\boldsymbol{u}_3 = \begin{bmatrix} P^* & Q^* & v_{\mathrm{Od}} & v_{\mathrm{Oq}} & i_{\mathrm{Ld}} & i_{\mathrm{Lq}} & i_{\mathrm{Od}} & i_{\mathrm{Oq}} \end{bmatrix}^{\mathrm{T}}$. However, because of the form of (8), the inputs cannot be included as linear terms into the state-space model of the system; and therefore this model takes the form $\dot{\boldsymbol{x}}_3 = \boldsymbol{A}_3\boldsymbol{x}_3 + \boldsymbol{R}_3(\boldsymbol{u}_3)$. The full equation is as follows

$$\dot{\boldsymbol{x}}_3 = \begin{bmatrix} -\sqrt{2}\omega_{\mathrm{c}} & 0 & \omega_{\mathrm{c}}^2 & 0 \\ 0 & -\sqrt{2}\omega_{\mathrm{c}} & 0 & \omega_{\mathrm{c}}^2 \\ -1 & 0 & 0 & 0 \\ 0 & -1 & 0 & 0 \end{bmatrix} \begin{bmatrix} i^*_{\mathrm{Ld}} \\ i^*_{\mathrm{Lq}} \\ q_{3\mathrm{d}} \\ q_{3\mathrm{q}} \end{bmatrix} + \boldsymbol{R}_3(\boldsymbol{u}_3) \tag{13}$$

where $\boldsymbol{R}_3(\boldsymbol{u}_3)$ is the nonlinear function of the input variables

$$\boldsymbol{R}_3(\boldsymbol{u}_3) = \begin{bmatrix} 0 \\ 0 \\ i^{\Sigma}_{\mathrm{d}} \\ i^{\Sigma}_{\mathrm{q}} \end{bmatrix} = \begin{bmatrix} 0 \\ 0 \\ \dfrac{v_{\mathrm{Od}}P^* - v_{\mathrm{Oq}}Q^*}{v^2_{\mathrm{Od}} + v^2_{\mathrm{Oq}}} + i_{\mathrm{Ld}} - i_{\mathrm{Od}} \\ \dfrac{v_{\mathrm{Oq}}P^* + v_{\mathrm{Od}}Q^*}{v^2_{\mathrm{Od}} + v^2_{\mathrm{Oq}}} + i_{\mathrm{Lq}} - i_{\mathrm{Oq}} \end{bmatrix} \tag{14}$$

The output vector for the power regulator is composed of the two reference currents $\boldsymbol{y}_3 = \begin{bmatrix} i^*_{\mathrm{Ld}} & i^*_{\mathrm{Lq}} \end{bmatrix}$.

2.4 State-space model of the current controller

The current controller indicated in Fig. 1 is implemented as a pair of PI controllers together with cross-axis decoupling terms and feed-forward terms for the connection voltage. Because the inverter represents (on average) a gain equal to the DC link voltage, it is desirable to include a division by the DC link voltage so that the inverter remains a normalised gain term, even if the DC link voltage varies. The controller block diagram is shown in Fig. 4.

From Fig. 4, the following equations can be obtained

$$v^*_{\mathrm{Id}} = v_{\mathrm{Od}} - \omega L i_{\mathrm{Lq}} + K^{\mathrm{d2}}_P i^{\mathrm{err}}_{\mathrm{Ld}} + K^{\mathrm{d2}}_I \int i^{\mathrm{err}}_{\mathrm{Ld}}\,\mathrm{d}t \tag{15}$$

$$v^*_{\mathrm{Iq}} = v_{\mathrm{Oq}} - \omega L i_{\mathrm{Ld}} + K^{\mathrm{q2}}_P i^{\mathrm{err}}_{\mathrm{Ld}} + K^{\mathrm{q2}}_I \int i^{\mathrm{err}}_{\mathrm{Lq}}\,\mathrm{d}t \tag{16}$$

The frequency (ω) is taken from the PLL and is treated as an input, here.

Once again, new variables are introduced to obtain the state-space model: $q^{\mathrm{err}}_{\mathrm{Ld}} = \int i^{\mathrm{err}}_{\mathrm{Lq}}\,\mathrm{d}t$ and $q^{\mathrm{err}}_{\mathrm{Lq}} = \int i^{\mathrm{err}}_{\mathrm{Lq}}\,\mathrm{d}t$. The state and input vectors of the current controller are given by (17) and (18), respectively.

$$\boldsymbol{x}_4 = \begin{bmatrix} q^{\mathrm{err}}_{\mathrm{Ld}} & q^{\mathrm{err}}_{\mathrm{Lq}} \end{bmatrix}^{\mathrm{T}} \tag{17}$$

$$\boldsymbol{u}_4 = \begin{bmatrix} i^{\mathrm{err}}_{\mathrm{Ld}} & i^{\mathrm{err}}_{\mathrm{Lq}} & i_{\mathrm{Ld}} & i_{\mathrm{Lq}} & v_{\mathrm{Od}} & v_{\mathrm{Oq}} & \omega \end{bmatrix}^{\mathrm{T}} \tag{18}$$

The state-space model is in standard linear form, $\dot{\boldsymbol{x}}_4 = \boldsymbol{A}_4\boldsymbol{x}_4 + \boldsymbol{B}_4\boldsymbol{u}_4$, but because the two new states of this sub-system do not involve internal feedback, the $\boldsymbol{A}$ matrix is zero. The model is given in (19)

$$\dot{\mathbf{x}}_4 = \begin{bmatrix} 0 & 0 \\ 0 & 0 \end{bmatrix} \begin{bmatrix} q^{\mathrm{err}}_{\mathrm{Ld}} \\ q^{\mathrm{err}}_{\mathrm{Lq}} \end{bmatrix} + \begin{bmatrix} 1 & 0 & 0 & 0 & 0 & 0 & 0 \\ 0 & 1 & 0 & 0 & 0 & 0 & 0 \end{bmatrix} \times \begin{bmatrix} i^{\mathrm{err}}_{\mathrm{Ld}} \\ i^{\mathrm{err}}_{\mathrm{Lq}} \\ i_{\mathrm{Ld}} \\ i_{\mathrm{Lq}} \\ v_{\mathrm{Od}} \\ v_{\mathrm{Oq}} \\ \omega \end{bmatrix} \tag{19}$$

The output equation is in standard form except for the division by the DC link voltage

$$\boldsymbol{y}_4 = \frac{1}{v_{\mathrm{DC}}}(\boldsymbol{C}\boldsymbol{x} + \boldsymbol{D}\boldsymbol{u} + \boldsymbol{S}(\boldsymbol{u}))$$

$$\boldsymbol{y}_4 = \frac{1}{v_{\mathrm{DC}}}\left(\begin{bmatrix} K^{\mathrm{d2}}_{\mathrm{T}} & 0 \\ 0 & K^{\mathrm{q2}}_{\mathrm{T}} \end{bmatrix} \begin{bmatrix} q^{\mathrm{err}}_{\mathrm{Ld}} \\ q^{\mathrm{err}}_{\mathrm{Lq}} \end{bmatrix} + \begin{bmatrix} K^{\mathrm{d2}}_{\mathrm{P}} & 0 & 0 & 0 & 1 & 0 & 0 \\ 0 & K^{\mathrm{q2}}_{\mathrm{P}} & 0 & 0 & 0 & 1 & 0 \end{bmatrix} \begin{bmatrix} i^{\mathrm{err}}_{\mathrm{Ld}} \\ i^{\mathrm{err}}_{\mathrm{Lq}} \\ i_{\mathrm{Ld}} \\ i_{\mathrm{Lq}} \\ v_{\mathrm{od}} \\ v_{\mathrm{Oag}} \\ \omega \end{bmatrix} + \begin{bmatrix} -\omega L i_{\mathrm{Lq}} \\ \omega L i_{\mathrm{Ld}} \end{bmatrix} \right) \tag{20}$$

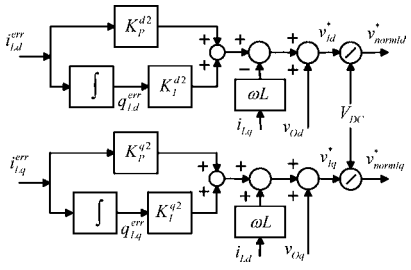

Fig. 4 *Model for the current controller*

2.5 State-space model of the inverter

The inverter itself is a switch-mode circuit and, for the purpose of this model development, it is assumed that the switching frequency is sufficiently high that the switching action itself does no affect the evolution of the states, and the state-space averaging can be applied. In other words, the switching frequency ripple of states such as the inductor currents can be ignored without significantly affecting the accuracy with which the average inductor current is predicted. It is expected that the passive low-pass filter at the output of the inverter will have been chosen to attenuate switching frequency ripple to acceptable levels. As switching frequencies of commercial DG inverters continue to improve, this approximation becomes better. There may be some high-power inverters with low switching frequencies (<1 kHz) where the physical size and the cost of the filter have been constrained and where the state-space averaging assumptions are not strictly valid.

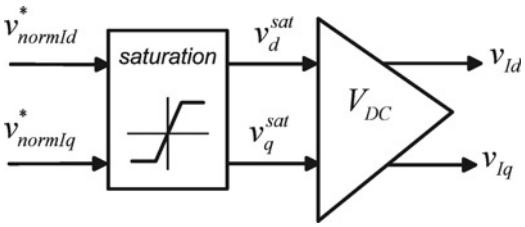

Fig. 5 *Simplified model of the inverter*

With the switching action of the inverter neglected, the model of the inverter can be simplified to a saturated voltage gain, as shown in Fig. 5.

Saturation arises because there is a finite DC-link voltage, which in turn produces a magnitude-constrained AC voltage at the output. Because the saturation function is a nonlinear element, it is not included in the linear differential equations. Voltage saturation is, however, an important characteristic of VSI and it should be modelled in time-step simulations, used to verify results from line-arised *s*-domain models. Saturation can be included in time-step simulations with if-then-else commands, as shown in Table 1.

The voltage gain model of the VSI in state-space variables is simply

$$\dot{x}_5 = [0] \tag{21}$$

The output is $y_5 = \begin{bmatrix} v_{\mathrm{Id}} & v_{\mathrm{Id}} \end{bmatrix}$

2.6 State-space model of LC filter and coupling impedance

Although the switching frequency ripple has been dismissed from the model, the passive low-pass filter must still be included in it. The selection of the inductors and capacitors of this filter involves some design compromise and the filter will have important dynamic effects down to quite low frequencies. This sub-system includes both the coupling inductance that is always present and any additional filter components. The coupling impedance might in reality be a coupling inductor or the leakage impedance of a coupling transformer. If this is indeed a coupling inductor, the LC filter becomes a LCL filter. How to design the output filters is out of the scope of this paper; detailed analyses of these filters can be found in [24, 25].

The LC filter (assumed symmetric)in the abc reference frame is shown in Fig. 6.

The equations describing phase a of the filter are presented in (22)–(24).

Table 1: Computer-based model of saturation

Saturation
if $(v^*_{\mathrm{normId}})^2 + (v^*_{\mathrm{normId}})^2 \geq \frac{1}{2}$
$\theta = \tan^{-1} \frac{v^*_{\mathrm{normIq}}}{v^*_{normId}}$
$v_d^{\mathrm{sat}} = \frac{1}{\sqrt{2}} \cos(\theta)$
$v_q^{\mathrm{sat}} = \frac{1}{\sqrt{2}} \sin(\theta)$
else $v_{\mathrm{d}}^{\mathrm{sat}} = v^*_{\mathrm{normId}}$
$v_{\mathrm{q}}^{\mathrm{sat}} = v^*_{\mathrm{normIq}}$
End

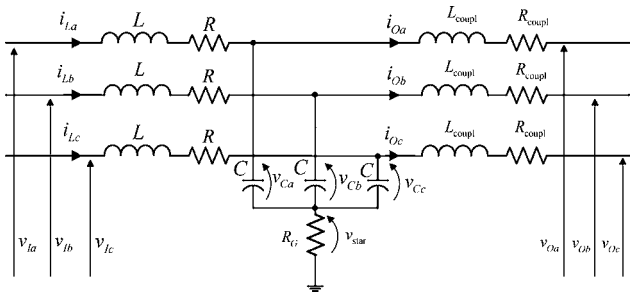

Fig. 6 *LC filter and load*

$$v_{\mathrm{Ia}} = i_{\mathrm{La}} R + L \frac{\mathrm{d}i_{\mathrm{La}}}{\mathrm{d}t} + v_{\mathrm{Ca}} + v_{\mathrm{star}} \tag{22}$$

$$v_{\mathrm{Oa}} = v_{\mathrm{Ca}} + v_{\mathrm{star}} - L_{\mathrm{coupl}} \frac{\mathrm{d}i_{\mathrm{Oa}}}{\mathrm{d}t} - i_{\mathrm{Oa}} R_{\mathrm{coupl}} \tag{23}$$

$$C \frac{\mathrm{d}v_{\mathrm{Ca}}}{\mathrm{d}t} = i_{\mathrm{La}} - i_{\mathrm{Oa}} \tag{24}$$

$$v_{\mathrm{star}} = 3R_G(i_{\mathrm{La}} - i_{\mathrm{Oa}}) \tag{25}$$

To create a general filter model, the star-point of the capacitors is connected to ground by an impedance. Selecting a low value impedance would model a four-wire filter and a high-value impedance would model a three-wire filter. The input, output and state vectors of the filter in dq form are

$$\boldsymbol{u}_6 = \begin{bmatrix} v_{\mathrm{Id}} & v_{\mathrm{Iq}} & v_{\mathrm{I_O}} & v_{\mathrm{O_d}} & v_{\mathrm{O_q}} & v_{\mathrm{O_o}} & \omega \end{bmatrix}^{\mathrm{T}}$$

$$\boldsymbol{y}_6 = \begin{bmatrix} i_{\mathrm{Ld}} & i_{\mathrm{Lq}} & i_{\mathrm{Lo}} & i_{\mathrm{Od}} & i_{\mathrm{O_q}} & i_{\mathrm{O_o}} \end{bmatrix}^{\mathrm{T}}$$

$$\boldsymbol{x}_6 = \begin{bmatrix} i_{\mathrm{Ld}} & i_{\mathrm{Lq}} & i_{\mathrm{L_O}} & v_{\mathrm{Cd}} & v_{\mathrm{C_q}} & v_{\mathrm{C_o}} & i_{\mathrm{Od}} & i_{\mathrm{O_q}} & i_{\mathrm{O_O}} \end{bmatrix}^{\mathrm{T}}$$

The matrices $\boldsymbol{A}_6$, $\boldsymbol{B}_6$ and $\boldsymbol{R}_6$ in the state-space model $\dot{\boldsymbol{x}}_6 = \boldsymbol{A}_6 \boldsymbol{x}_6 + \boldsymbol{B}_6 \boldsymbol{u}_6 + \boldsymbol{R}_6(\boldsymbol{x}_6, \boldsymbol{u}_6)$ are found to be

$$\boldsymbol{A}_6 = \begin{bmatrix} \frac{-R}{L} & 0 & 0 & \frac{-1}{L} & 0 \\ 0 & \frac{-R}{L} & 0 & 0 & \frac{-1}{L} \\ 0 & 0 & \frac{-3R_G - R}{L} & 0 & 0 \\ \frac{1}{C} & 0 & 0 & 0 & 0 \\ 0 & \frac{1}{C} & 0 & 0 & 0 \\ 0 & 0 & \frac{1}{C} & 0 & 0 \\ 0 & 0 & 0 & \frac{1}{L_{\mathrm{coupl}}} & 0 \\ 0 & 0 & 0 & 0 & \frac{1}{L_{\mathrm{coupl}}} \\ 0 & 0 & 0 & 0 & 0 \end{bmatrix} \tag{26}$$

$$\begin{bmatrix} 0 & 0 & 0 & 0 \\ 0 & 0 & 0 & 0 \\ \frac{-1}{L} & 0 & 0 & \frac{3R_G}{L} \\ 0 & \frac{-1}{C} & 0 & 0 \\ 0 & 0 & \frac{-1}{C} & 0 \\ 0 & 0 & 0 & \frac{-1}{C} \\ 0 & \frac{-R_{\mathrm{coupl}}}{L_{\mathrm{coupl}}} & 0 & 0 \\ 0 & 0 & \frac{-R_{\mathrm{coupl}}}{L_{\mathrm{coupl}}} & 0 \\ \frac{3R_G}{L_{\mathrm{coupl}}} & 0 & 0 & \frac{-3R_G - R_{\mathrm{coupl}}}{L_{\mathrm{coupl}}} \end{bmatrix}$$

$$\boldsymbol{B}_6 = \begin{bmatrix} \frac{1}{L} & 0 & 0 & 0 & 0 & 0 & 0 \\ 0 & \frac{1}{L} & 0 & 0 & 0 & 0 & 0 \\ 0 & 0 & \frac{1}{L} & 0 & 0 & 0 & 0 \\ 0 & 0 & 0 & 0 & 0 & 0 & 0 \\ 0 & 0 & 0 & 0 & 0 & 0 & 0 \\ 0 & 0 & 0 & 0 & 0 & 0 & 0 \\ 0 & 0 & 0 & \frac{-1}{L_{\text{coupl}}} & 0 & 0 & 0 \\ 0 & 0 & 0 & 0 & \frac{-1}{L_{\text{coupl}}} & 0 & 0 \\ 0 & 0 & 0 & 0 & 0 & \frac{-1}{L_{\text{coupl}}} & 0 \end{bmatrix}$$

$$\mathbf{R}_6 = \begin{bmatrix} \omega i_{\text{Lq}} \\ -\omega i_{\text{Ld}} \\ 0 \\ \omega v_{\text{Cq}} \\ -\omega v_{\text{Cd}} \\ 0 \\ \omega i_{\text{Oq}} \\ -\omega i_{\text{Od}} \\ 0 \end{bmatrix} \tag{27}$$

The output matrix is

$$\boldsymbol{C}_6 = \begin{bmatrix} 1 & 0 & 0 & 0 & 0 & 0 & 0 & 0 & 0 \\ 0 & 1 & 0 & 0 & 0 & 0 & 0 & 0 & 0 \\ 0 & 0 & 1 & 0 & 0 & 0 & 0 & 0 & 0 \\ 0 & 0 & 0 & 0 & 0 & 0 & 1 & 0 & 0 \\ 0 & 0 & 0 & 0 & 0 & 0 & 0 & 1 & 0 \\ 0 & 0 & 0 & 0 & 0 & 0 & 0 & 0 & 1 \end{bmatrix} \tag{28}$$

3 Complete model

Fig. 7 is a re-drawing of Fig. 1, but with the state variables of each sub-system identified ready to form the overall model of a current-controlled inverter (CCI) that was envisaged in (1). The inputs of the system can readily be assembled into the input vector ($\boldsymbol{u}$) given by (29).

$$\boldsymbol{u}_{\text{CCI}} = \begin{bmatrix} V_{\text{DC}} & v_{\text{Oa}} & v_{\text{Ob}} & v_{\text{Oc}} & P^* & Q^* \end{bmatrix}^{\text{T}} \tag{29}$$

The state variables also need to be combined into a single state vector as given by (30). The first two state variables, θ and Φ_{PLL}, are contributed by the PLL system. Four state variables arise from the two second-order Butterworth filters in the power controller: i_{Ld}^*, i_{Lq}^*, $q_{3\text{d}}$ and $q_{3\text{q}}$. Variables $q_{\text{Ld}}^{\text{err}}$ and $q_{\text{Lq}}^{\text{err}}$ are the result of the integrators in the current controller. The states, i_{Ld}, i_{Lq}, i_{Lo}, v_{Cd}, v_{Cq}, and v_{Co}, appear due to the reactive elements of LC filter and, finally, i_{Od}, i_{Oq} and i_{Oo} are contributed by the coupling reactance

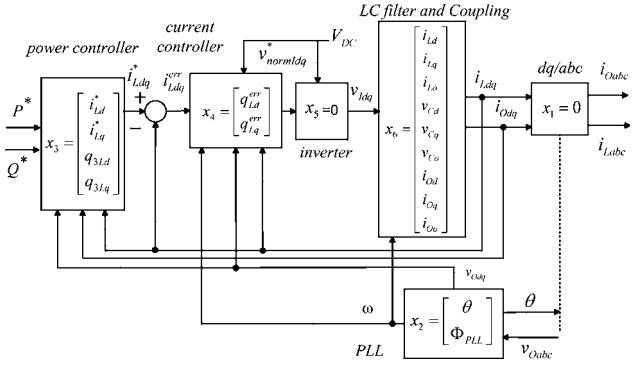

Fig. 7 *Topology of a CCI with the state vectors of each sub-system*

$$\boldsymbol{x}_{\text{CCI}} = \begin{bmatrix} \theta & \Phi_{\text{PLL}} & i_{\text{Ld}}^* & i_{\text{Lq}}^* & q_{3\text{Lq}} & q_{3\text{Lq}} & q_{\text{Ld}}^{\text{err}} & q_{\text{Lq}}^{\text{err}} \\ i_{\text{Ld}} & i_{\text{Lq}} & i_{\text{L}_\text{O}} & v_{\text{Cd}} & v_{\text{Cq}} & v_{\text{C}_\text{O}} & i_{\text{Od}} & i_{\text{Oq}} & i_{\text{O}_\text{o}} \end{bmatrix}^{\text{T}} \tag{30}$$

Matrix $\boldsymbol{A}_{\text{CCI}}$ for the whole system is obtained by combining together the $\boldsymbol{A}$ matrices of the PLL, the power controller, the current controller and the LC filter. This is because these four sub-systems are the only ones with the state variables in their models. Equation (31) illustrates how the matrices are combined

$$\boldsymbol{A}_{\text{CCI}} = \begin{bmatrix} [\boldsymbol{A}_2] & 0 & 0 & 0 \\ 0 & [\boldsymbol{A}_3] & 0 & 0 \\ 0 & 0 & [\boldsymbol{A}_4] & 0 \\ 0 & 0 & 0 & [\boldsymbol{A}_6] \end{bmatrix} \tag{31}$$

There are several simplifications to be made to the resulting matrix $\boldsymbol{A}_{\text{CCI}}$ to make it more compact. The inductor currents and their reference values occur in several places in the model such as in the error terms of the current controllers and as state variables in the power regulator. Furthermore, they are integrated to provide further state variables. The terms in $\boldsymbol{A}_3$ and $\boldsymbol{A}_4$ and in $\boldsymbol{R}_3$ and $\boldsymbol{B}_4$ can be simplified on combination to $\boldsymbol{A}_{34}$ and $\boldsymbol{R}_{34}$ as shown in (32)

$$\dot{\boldsymbol{x}}_{34} = \begin{bmatrix} -\sqrt{2\omega_c} & 0 & \omega_c^2 & 0 & 0 & 0 \\ 0 & -\sqrt{2\omega_c} & 0 & \omega_c^2 & 0 & 0 \\ -1 & 0 & 0 & 0 & 0 & 0 \\ 0 & -1 & 0 & 0 & 0 & 0 \\ 1 & 0 & 0 & 0 & 0 & 0 \\ 0 & 1 & 0 & 0 & 0 & 0 \end{bmatrix} \begin{bmatrix} i_{\text{Ld}}^* \\ i_{\text{Lq}}^* \\ q_{3\text{d}} \\ q_{3\text{q}} \\ q_{\text{Ld}}^{\text{err}} \\ q_{\text{Lq}}^{\text{err}} \end{bmatrix} + \boldsymbol{R}_{34}(\boldsymbol{u}_{34}) \tag{32}$$

$$\boldsymbol{R}_{34}(\boldsymbol{u}_{34}) = \begin{bmatrix} 0 \\ 0 \\ \frac{v_{\text{Od}}P^* - v_{\text{Oq}}Q^*}{v_{\text{Od}}^2 + v_{\text{Oq}}^2} + i_{\text{Lq}} - i_{\text{Od}} \\ \frac{v_{\text{Oq}}P^* - v_{\text{Od}}Q^*}{v_{\text{Od}}^2 + v_{\text{Oq}}^2} + i_{\text{Lq}} - i_{\text{Oq}} \\ -i_{\text{Ld}} \\ -i_{\text{Lq}} \end{bmatrix} \tag{33}$$

Furthermore, examination of $\boldsymbol{R}_{34}(\boldsymbol{u}_{34})$ reveals that i_{Ldq} and i_{Odq} are states of one of the other sub-systems and so the terms associated with them should appear in the $\boldsymbol{A}_{\text{CCI}}$ matrix of the complete system. Incorporating these modifications into (31) gives the complete matrix $\boldsymbol{A}_{\text{CCI}}$ defined in (34) for the CCI. The nonlinear dependencies found in the inverter system model, such as the products of states, and the input terms are collected in $\boldsymbol{R}_{\text{CCI}}(\boldsymbol{x}_{\text{CCI}}, \boldsymbol{u}_{\text{CCI}})$ as summarised in (35). An important nonlinearity to consider is in the calculation of the terms v_{Id} and v_{Iq}, which includes the possible application of the saturation limit.

$$
\boldsymbol{A}_{\mathrm{CCI}} = \begin{bmatrix}
0 & K_I^{\mathrm{PLL}} & 0 & 0 & 0 & 0 \\
0 & 0 & 0 & 0 & 0 & 0 \\
0 & 0 & -\sqrt{2}\omega_c & 0 & \omega_c^2 & 0 \\
0 & 0 & 0 & -\sqrt{2}\omega_c & 0 & \omega_c^2 \\
0 & 0 & -1 & 0 & 0 & 0 \\
0 & 0 & 0 & -1 & 0 & 0 \\
0 & 0 & 0 & 0 & 0 & 0 \\
0 & 0 & 0 & 0 & 0 & 0 \\
0 & 0 & 0 & 0 & 0 & 0 \\
0 & 0 & 0 & 0 & 0 & 0 \\
0 & 0 & 0 & 0 & 0 & 0 \\
0 & 0 & 0 & 0 & 0 & 0 \\
0 & 0 & 0 & 0 & 0 & 0 \\
0 & 0 & 0 & 0 & 0 & 0 \\
0 & 0 & 0 & 0 & 0 & 0 \\
0 & 0 & 0 & 0 & 0 & 0
\end{bmatrix}
$$

$$
\begin{bmatrix}
0 & 0 & 0 & 0 & 0 & 0 \\
0 & 0 & 0 & 0 & 0 & 0 \\
0 & 0 & 0 & 0 & 0 & 0 \\
0 & 0 & 0 & 0 & 0 & 0 \\
0 & 0 & 1 & 0 & 0 & 0 \\
0 & 0 & 0 & 1 & 0 & 0 \\
0 & 0 & -1 & 0 & 0 & 0 \\
0 & 0 & 0 & -1 & 0 & 0 \\
0 & 0 & \dfrac{-R}{L} & 0 & 0 & \dfrac{-1}{L} \\
0 & 0 & 0 & \dfrac{-R}{L} & 0 & 0 \\
0 & 0 & 0 & 0 & \dfrac{-3R_G - R}{L} & 0 \\
0 & 0 & \dfrac{1}{C} & 0 & 0 & 0 \\
0 & 0 & 0 & \dfrac{1}{C} & 0 & 0 \\
0 & 0 & 0 & 0 & \dfrac{1}{C} & 0 \\
0 & 0 & 0 & 0 & 0 & \dfrac{1}{L_{\mathrm{coupl}}} \\
0 & 0 & 0 & 0 & 0 & 0 \\
0 & 0 & 0 & 0 & 0 & 0
\end{bmatrix}
$$

$$
\begin{bmatrix}
0 & 0 & 0 & 0 & 0 \\
0 & 0 & 0 & 0 & 0 \\
0 & 0 & 0 & 0 & 0 \\
0 & 0 & 0 & 0 & 0 \\
0 & 0 & -1 & 0 & 0 \\
0 & 0 & 0 & -1 & 0 \\
0 & 0 & 0 & 0 & 0 \\
0 & 0 & 0 & 0 & 0 \\
0 & 0 & 0 & 0 & 0 \\
\dfrac{-1}{L} & 0 & 0 & 0 & 0 \\
0 & \dfrac{-1}{L} & 0 & 0 & \dfrac{3R_G}{L} \\
0 & 0 & \dfrac{-1}{C} & 0 & 0 \\
0 & 0 & 0 & \dfrac{-1}{C} & 0 \\
0 & 0 & 0 & 0 & \dfrac{-1}{C} \\
0 & 0 & \dfrac{-R_{\mathrm{coupl}}}{L_{\mathrm{coupl}}} & 0 & 0 \\
\dfrac{1}{L_{\mathrm{coupl}}} & 0 & 0 & \dfrac{-R_{\mathrm{coupl}}}{L_{\mathrm{coupl}}} & 0 \\
0 & \dfrac{-3R_G}{L_{\mathrm{coupl}}} & 0 & 0 & \dfrac{-3R_G - R_{\mathrm{coupl}}}{L_{\mathrm{coupl}}}
\end{bmatrix} \tag{34}
$$

$$
\boldsymbol{R}_{\mathrm{CCI}}(\boldsymbol{x}_{\mathrm{CCI}}, \boldsymbol{u}_{\mathrm{CCI}}) = \begin{bmatrix}
K_{\mathrm{P}}^{\mathrm{PPL}} v_{\mathrm{O_q}} \\
v_{\mathrm{O_q}} \\
0 \\
0 \\
\dfrac{v_{\mathrm{Od}} P^* - v_{\mathrm{Oq}} Q^*}{v_{\mathrm{Od}}^2 + v_{\mathrm{Oq}}^2} \\
\dfrac{v_{\mathrm{Oq}} P^* + v_{\mathrm{Od}} Q^*}{v_{\mathrm{Od}}^2 + v_{\mathrm{Oq}}^2} \\
0 \\
0 \\
\dfrac{1}{L} v_{\mathrm{Ld}} + \omega i_{\mathrm{Lq}} \\
\dfrac{1}{L} v_{\mathrm{Iq}} - \omega i_{\mathrm{Ld}} \\
0 \\
\omega v_{\mathrm{Cq}} \\
-\omega v_{\mathrm{Cd}} \\
0 \\
-\dfrac{1}{L_{\mathrm{coupl}}} v_{\mathrm{Od}} + \omega i_{\mathrm{Oq}} \\
-\dfrac{1}{L_{\mathrm{coupl}}} v_{\mathrm{Oq}} + \omega i_{\mathrm{Od}} \\
0
\end{bmatrix} \tag{35}
$$

The final task is to assemble the output vector for (1), which will normally be composed of the output currents. To aid the verification of the model, the filter inductor currents have also been included. These variables are in abc form and so are computed as a function of both the corresponding state variables in dq form and the state variable representing the angle of the dq–abc transformation, as described in (2). The DC link current could be added to this vector and (by assuming that the inverter itself is power conserving) calculated as an algebraic manipulation of the normalised inverter voltages and the inductor currents.

$$
\boldsymbol{y}_{\mathrm{CCI}} = \begin{bmatrix} i_{\mathrm{La}} & i_{\mathrm{Lb}} & i_{\mathrm{Lc}} & i_{\mathrm{Oa}} & i_{\mathrm{Ob}} & i_{\mathrm{Oc}} \end{bmatrix}^{\mathrm{T}} \tag{36}
$$

4 Validation examples

The state-space model relies on the development of many supporting equations and some modelling assumptions. To verify the state-space model, solutions generated by it were compared to solutions from a component and block level simulation in Simulink. The PLECS toolbox for Simulink was used to give component-level simulation of power electronic devices and other circuit elements. Both the state-space and Simulink models were set up with the parameters shown in Table 2.

4.1 Numerical solution of the state-space model

The state-space model can be used within general simulation systems or power-system specific software. For this validation, it was explicitly solved using numerical integration in a MATLAB script. There are several integration methods available for solving differential-algebraic equations. The partitioned-explicit solution method is chosen here, since a need to examine dynamics over a wide range of time-scales is not required. The simultaneous implicit solution would be preferred in that case [26]. The PE solution was implemented in MATLAB scripts using an explicit 4th-order Runge–Kutta formula.

Table 2: Simulation setup

parameter		value
nominal phase voltage		240 V
grid frequency		50 Hz
coupling impedance		$(0.131 + j\omega 0.96 \times 10^{-3})\ \Omega$
DC bus voltage		1000 V
filter	inductance	1.35 mH
	capacitance	50 μF
	resistance	0.056 Ω
switching frequency		8 kHz
reference active power		10 kW
reference reactive power		5 kVar
current controller	proportional gain in branch d K_P^d	1
	integral gain in branch d K_I^d	460
	proportional gain in branch q K_P^q	1
	integral gain in branch q K_I^q	460
PLL	proportional gain K_P	2.1
	Integral gain K_I	5000

4.2 Component-level comparator model

Fig. 8 shows the overall Simulink model of the grid-connected inverter. The 'PLL', 'Power Controller' and 'Current control' correspond to Figs. 2–4, respectively. The block 'abc–dq' implements the *dq* transformation given in (4), and the block 'space vector modulation (SVM)' contains a MATLAB script, which produces the power transistor gate signals from 2-axis voltages in stationary reference frame (v_α and v_β) using the SVM technique. (The SVM process and the transistor switching action were explicitly excluded from the the state-space model.) The gate signals are then applied to an inverter circuit created in the PLECS extension to Simulink as shown in Fig. 9.

5 Comparison of results

5.1 Initial transient

At start up, there is an initial transient as the controllers act to establish the requested power flow. Both models were given power references of $P^* = 10$ kW, $Q^* = 5$ kVAr. The inductor currents in abc form are shown in Fig. 10*a*. The upper graph shows the results from the PLECS/Simulink model and the lower graph shows those from the state-space model. It is clear that both the initial transient and steady-state sinusoidal currents present the same evolution in time, in each case, but that the Simulink model has a high-frequency ripple superimposed on the basic current waveform. This is the ripple arising from the switching action of the inverter and was explicitly excluded from the state-space model.

The inductor currents are internal states and will not normally be used as outputs of the model in a system study. Fig. 10*b* shows the output currents, that is, the currents that flow in the grid connection (again in abc form); here the PLECS/Simulink results show very little switching frequency ripple because the LC filter has attenuated these components. This justifies the argument presented in Section 2.5 that at the connection point, the switching ripple is relatively small and in most cases it can be neglected. The lower graph in Fig. 10*b* confirms that the state-space model gives an accurate representation of the system. The output powers from both models are presented in Fig. 11 and again show good agreement.

5.2 Step change in load

A series of further tests were conducted to illustrate the type of study that the state-space model facilitates. The response of the inverter to changes in power reference is an important performance criterion. Here it was tested with a series of step changes. The initial reference values of the active and reactive powers were 10 kW and 5 kVAr. The active power was stepped up to 20 kW at 0.1 s, and stepped down to 10 kW at 0.35 s. The reactive power was stepped down to 2 kVAr at 0.2 s, and stepped up to 5 kVAr at 0.45 s. The

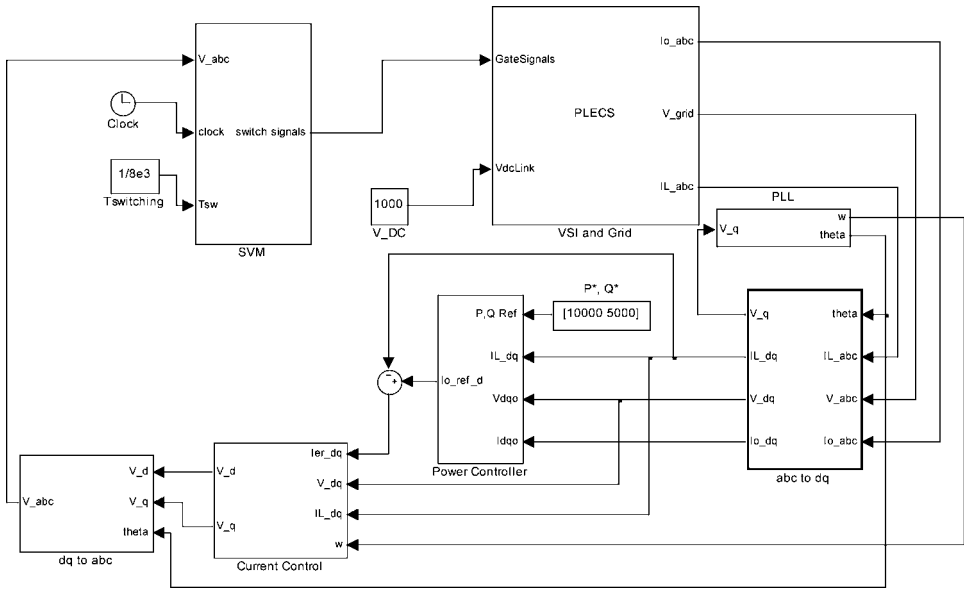

Fig. 8 *Simulink model of current controlled VSI with its ancillary circuits*

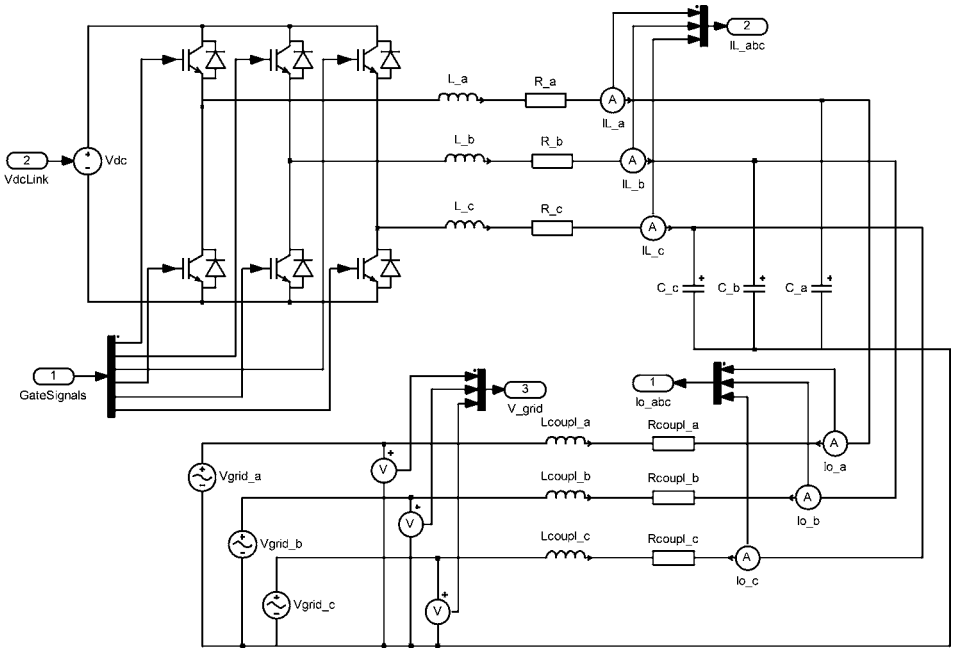

Fig. 9 *PLECS model of inverter, LC filter and coupling impedance*

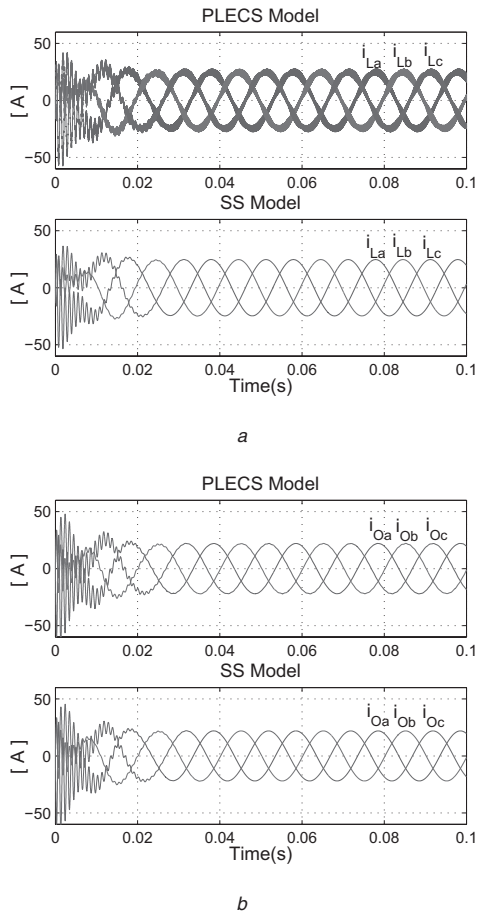

Fig. 10 *Behaviour during the initial transient in the abc reference frame*

a Inductor currents
b Output currents

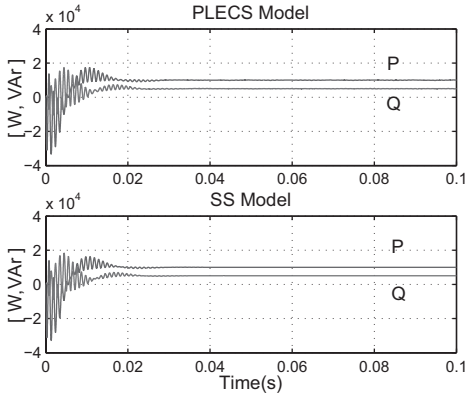

Fig. 11 *Output power*

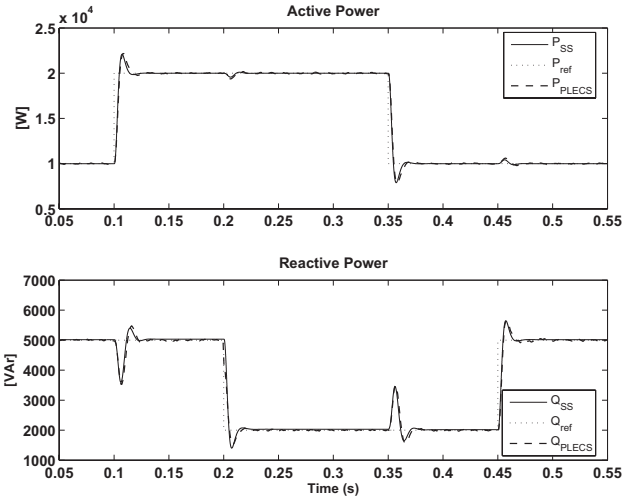

Fig. 12 *Reference and actual active and reactive power*

resulting output powers of the system together with the reference powers are shown in Fig. 12 (the initial 0.05 s containing the start-up transient is not shown). It can be seen that the response to the changes in reference values is fast and without significant overshoot, but that there is some coupling between the active and reactive power (e.g. the step change of P at 0.1 results in a negative excursion in Q), which might be tackled through changes to the current controller.

6 Conclusions

An appropriate level of detail is needed in a model for each purpose to which it is put. A state-space model has been presented that enables transient stability of a grid connected inverter to be studied. The model is in state-space form and specifically avoids simulation of switching frequency effects. It has been shown to capture the important dynamics of the passive output filter, the current controllers, the filter in the power reference to current reference conversion and the controller that establishes phase-locking. This phase-locked and current-controlled form of inverters are common for DG connected to relatively strong grids. The model has been built up in stages, or subsystems, so that it can be related to practical implementations of inverters. The state-space form allows coupling of this model to standard models of distribution grids and coupling of several inverters in one system. The state vector has a similar form to the state vector of standard models of rotating machines. Thus, full dynamic models of complex systems can be built and stability of the system assessed through either time-domain technique or, after linearisation, frequency-domain techniques. The model can also be coupled to models of the original DC energy source through the DC-link port provided. Participation analysis will allow identification of appropriate inverter features that influence oscillatory modes of a system. Through experience with various inverter implementations it will be possible to establish general rules for enhancing the stability of networks that include inverter-interfaced DG.

7 References

1 Agbossou, A., Rasoanarivo, I., and Davat, B.: 'A comparative study of high power IGBT model behaviour in voltage source inverter'. 'IEEE 27th Annual Power Electronics Specialist Conf. (PESC), vol. 1, 1996 pp. 56–61

2 Mihailovic, Z., Prasad, H., and Borojevic, D.: 'Computer modeling and analysis of VSI fed permanent magnet synchronous motor drive systems with adjustable levels of complexity'. 12th Annual Applied Power Electronics Conf. and Exposition (APEC), Atlanta, GA, 1997, vol. 2, pp. 728–735

3 Salazar, L., and Joos, G.: 'PSpice simulation of three-phase inverters by means of switching functions', *IEEE Trans. Power Elect.*, 1994, **9**, (1), pp. 35–42

4 Lee, B., and Ehsani, M.: 'A simplified functional model for 3-phase voltage source inverter using switching function concept'. The 25th Annual Conf. on Industrial Electronics Society (IECON), San Jose, CA, 1999, vol. 1, pp. 462–467

5 Alimeling, J., and Hammer, W.: 'Plecs-piece-wise linear electrical circuit simulation for simulink'. Proc. IEEE 1999 Int. Conf. on Power Electronics and Drive Systems, 1999, vol. 1, pp. 355–360

6 Kassakian, J.G., Schlecht, M.F., and Verghese, G.C.: 'Principles of power electronics'. (Addison-Wesley, 1991)

7 Karagiannis, D., Mendes, E., Astolfi, A., and Ortega, R.: 'An experimental comparison of several PWM controllers for a single-phase AC–DC converter', *IEEE Trans. Control Sys. Technol.*, 2003, **11**, pp. 940–947

8 Hiti, S., Boroyevich, D., and Cuadros, C.: 'Small-signal modeling and control of three-phase PWM converters'. Industry applications society annual meeting, 1994, vol. 2, pp. 1143–1150

9 Blasko, V., and Kaura, V.: 'A new mathematical model and control of a three-phase AC–DC voltage source converter', *IEEE Trans. Power Elect.*, 1997, **12**, (1), pp. 116–123

10 Lehn, P.: 'Exact modeling of the voltage source converter', *IEEE Trans. Power Deliv.*, 2002, **17**, (1), pp. 217–222

11 Bordonau, J., Cosan, M., Borojevic, D., Mao, H., and Lee, F.: 'A state-space model for the comprehensive dynamic analysis of three-level voltage-source inverters'. IEEE 28th Annual Power Electronics Specialists Conf., St. Louis, MO, 1997, vol. 2, pp. 942–948

12 Celanovic, N., Lee, D.-H., Peng, D., Borojevic, D., and Lee, F.: 'Control design of three-level voltage source inverter for SMES power conditioning system'. IEEE 30th Annual Power Electronics Specialists Conf. (PESC), Charleston, SC, 1999, vol. 2, pp. 613–618

13 Fritsche, C., Schmitt, P., and Gerster, C.: 'Microprocessor-based control system for high-speed three-phase voltage source inverters with lc output filter'. IEEE 30th Annual Power Electronics Specialists Conf. (PESC), Charleston, SC, 1999, vol. 1, pp. 527–532

14 Alepuz, S., Gilabert, A., Arguelles, E., Bordonau, J., and Peracaula, J.: 'A new approach for the connection of a three-level inverter to the power grid for applications in solar energy conversion'. IEEE 28th Annual Conf. on the Industrial Electronics Society (IECON), 2002, vol. 4, pp. 3285–3290

15 Han, B., Karady, G., Park, J., and Moon, S.: 'Interaction analysis model for transmission static compensator with EMTP', *IEEE Trans. Power Deliv.*, 1998, **13**, (4), pp. 1297–1302

16 Abdel-Rahim, N., and Quaicoe, J.: 'Small-signal model and analysis of a multiple feedback control scheme for three-phase voltage-source UPS inverters'. IEEE 27th Annual Power Electronics Specialists Conf. (PESC), Baveno, 1996, vol. 1, pp. 188–194

17 Lehn, P., and Irvani, M.: 'Discrete time modeling and control of the voltage source converter for improved disturbance rejection', *IEEE Trans. Power Elect.*, 1999, **14**, (6), pp. 1028–1036

18 Alepuz, S., Bordonau, J., and Peracaula, J.: 'Dynamic analysis of three-level voltage-source inverters applied to power regulation'. IEEE 30th Annual Power Electronics Specialists Conf., Charleston, SC, 1999, vol. 2, pp. 721–726

19 Alepuz, S., Bordonau, J., and Peracaula, J.: 'A novel control approach of three-level VSIs using a LQR-based gain-scheduling technique'. Power Electronics Specialists Conf., 2000. PESC 00. 2000 IEEE 31st Annual, 2000, vol. 2, pp. 743–748

20 Guerrero, J., de Vicuna, L., Matas, J., Castilla, M., and Miret, J.: 'A wireless controller to enhance dynamic performance of parallel inverters in distributed generation systems', *IEEE Trans. Power Elect.*, 2004, **19**, (5), pp. 1205–1213

21 Prodanovic, M., and Green, T.: 'Control and filter design of three-phase inverters for high power quality grid connection', *IEEE Trans. Power Elect.*, 2003, **18**, (1), pp. 373–380

22 Prodanovic, M.: 'Power quality and control aspects of parallel connected inverters in distributed generation', PhD Dissertation Thesis, Imperial College, University of London, January 2004

23 Kaura, V., and Blasko, V.: 'Operation of a phase locked loop system under distorted utility conditions'. Proc. Annual Applied Power Electronics Conf., April 1996, vol. 2, pp. 703–708

24 Liserre, M., Blaabjerg, F., and Hansen, S.: 'Design and control of an lcl-filter-based three-phase active rectifier', *IEEE Trans. Ind. Appl.*, 2005, **41**, (5), pp. 1281–1291

25 Bolsens, B., De Brabandere, K., Van den Keybus, J., Driesen, J., and Belmans, R.: 'Model-based generation of low distortion currents in grid-coupled pwm-inverters using an lcl output filter', *IEEE Trans. Power Elect.*, 2006, **21**, (4), pp. 1032–1040

26 Sayer, P.W., and Pai, M.: 'Power system dynamics and stability' (Prentice-Hall, New Jersey, 1998)